JOURNAL OF MATERIALS SCIENCE 27 (1992) 5653–5660

Wettability of nickel alloys by Ni–Si–B fillers: influence of substrate oxide reduction and isothermal solidification

W. F. GALE, E. R. WALLACH
Department of Materials Science and Metallurgy, University of Cambridge, UK

The process of wetting of nickel and nickel–chromium substrates by nickel–silicon–boron filler metals is examined. In this system, wetting behaviour is dominated by interactions between the filler metal and the oxide layer on the substrate (which is not completely removed during conventional vacuum brazing). Boron emanating from the filler metal reduces this residual oxide. The extent of wettability is controlled by the onset of isothermal solidification which is a consequence of the removal of boron from the filler metal due to the reaction with the substrate oxide layer.

1. Introduction

The process of isothermal solidification has received considerable attention in the literature as it forms the basis of transient liquid phase (TLP) bonding [1–4]. In TLP bonding, interdiffusion between the substrate and filler metal results in the removal of the liquid phase during holding at the bonding temperature. Thus, most TLP studies have been concerned with the progression rather than the onset of isothermal solidification. In contrast, when considering the extent of wettability in high-temperature brazing, it is the onset rather than the progression of isothermal solidification that is of importance. In previous work [5], it was suggested that the onset of isothermal solidification of Ni–Si–B fillers on Ni–Cr substrates occurs as a result of boron removal from the filler due to both diffusion into the substrate and reaction with the substrate oxide layer. A study of this phenomenon is described in this paper.

In order to examine further the interaction between reduction of the substrate oxide layer and the onset of isothermal solidification, a number of areas need to be addressed:

(a) evidence of the nature of the oxide layer in the absence of oxide reduction by filler metal constituents;

(b) examination of the nature of the oxide reduction reaction(s);

(c) quantification of the interaction between oxide reduction and isothermal solidification (involving prediction of the time taken to initiate isothermal solidification);

(d) anomalous spreading behaviour observed at high brazing temperatures (above 1150 °C).

These aspects are considered in this paper.

2. Experimental procedure

Examination of the spreading of a Ni–4.5 wt % Si–3.2 wt % B filler (AWS designation: BNi-3) was conducted using discs (each 1 mm nominal diameter and 51 μm thick) preplaced on a range of nickel and nickel–chromium substrates (Ni–0, 5, 10, 15 and 20 wt % Cr). A brazing temperature of 1150 °C and a vacuum of 10^{-5} mbar was employed for this work.

Dynamic observations of the spreading process were carried out by using hot-stage light microscopy together with video recording. This technique was used to determine both the average diameter of the droplets and also the displacement of individual liquid–solid interfaces as a function of holding time at the brazing temperature. Of the two types of measurements made, average diameters were employed when comparison of different conditions was required as they demonstrated a high degree of repeatability (see Section 3.3). In contrast, displacement measurements provided more detailed information on the stages involved in spreading; however, these results varied from one solid–liquid interface to another within a particular sample. Hence, average diameter rather than displacement measurements were employed when accurate comparisons of different samples were required.

In addition to the dynamic spreading tests, sessile drop spread tests and further microscopy samples were prepared using holding times of 20 min at temperatures between 1065 and 1150 °C, under a range of vacuums between 5×10^{-6} and 7×10^{-5} mbar. At the higher pressures, the residual atmosphere was air-rich so that the behaviour of thicker oxide layers could be studied. This atmosphere was produced by pumping the furnace to below 5×10^{-6} mbar and then leaking air back into the chamber to achieve the working pressure.

Scanning electron microscopy (SEM) of the oxide layers formed on the substrates and of the regions of reaction around the braze droplets was conducted

0022-2461

using Camscan S2 and S4 instruments. These results were correlated with analytical investigations employing laser microprobe mass spectrometry (LAMMS) in a Cambridge Mass Spectrometry LIMA 2A instrument, energy dispersive X-ray spectroscopy (EDS) using a Link systems 860 analyser attached to the Camscan S4, and X-ray diffraction (XRD) in a Philips vertical diffractometer and a Huber Guinier camera.

3. Results and discussion

3.1. Oxide formation and deoxidation

When considering the possible influence, on wettability, of reduction of the substrate oxide by filler-metal constituents, it is necessary first to examine the stability of the substrate oxide layer in the absence of the filler. In this context, the tests conducted at 7×10^{-5} mbar (in an air-rich atmosphere) were particularly useful, because these conditions produced sufficient oxide to allow examination and hence phase identification using X-ray diffraction, together with data from EDS and LAMMS analyses. Results were obtained at 1065 and 1150 °C and are now discussed.

3.1.1. Oxide formation

Heating to the brazing temperature of either 1065 or 1150 °C without holding for any length of time produced the following results for the nickel and Ni–Cr substrates. NiO was present on all of the samples studied. However, the extent of NiO formation varied with substrate chromium content. Based on qualitative comparisons of XRD peak strengths, the greatest extent of NiO formation took place on the Ni–5% Cr substrate, and this was followed by that on the pure nickel substrate. Chromium addition above 5% (i.e. 10%, 15% and 20%) gradually decreased the extent of NiO formation (although an NiO layer remained present on the sample surface, see Fig. 1). The precipitation of Cr_2O_3 and $NiCr_2O_4$ (to some extent) occurred on all of the Ni–Cr substrates. The extent of Cr_2O_3 precipitation increased with chromium additions and reached a maximum on the Ni–20% Cr substrates.

It might appear surprising, at first sight, that the results of the oxidation experiments in vacuum described above are similar to those obtained from oxidation in air (e.g. [6, 7]) in terms of the behaviour with substrate chromium content. However, it must be borne in mind that as long as NiO remains stable (which is clearly the case here), Cr_2O_3 formation takes place in the substrate below the NiO layer and so is effectively isolated from the atmosphere. Hence the formation of Cr_2O_3 will be influenced firstly by the activity of chromium in the substrate and secondly by the maximum oxygen content in the substrate below the NiO layer. Under the experimental conditions used, both are independent of the pressure of the atmosphere above the substrate and hence similar behaviour with different chromium contents in the substrate would be expected. Note, however, that the actual rate of oxidation should be considerably reduced in vacuum compared with that in air.

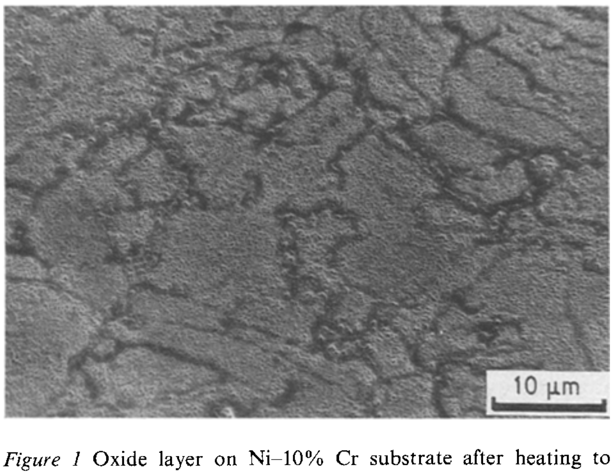

Figure 1 Oxide layer on Ni–10% Cr substrate after heating to 1065 °C in a 7×10^{-5} mbar vacuum.

In summary, the composition of the oxide layers under vacuums of around 10^{-5} mbar follows that observed in air although the actual amount of oxide present would be expected to be reduced.

3.1.2. Deoxidation phenomena

Following 20 min holding at the brazing temperature (of 1065 or 1150 °C), the amount of NiO present in the oxide layer was considerably reduced on all of the samples investigated to such an extent that this phase could no longer be detected using XRD. However, LAMMS and/or EDS studies of both the nickel and Ni–Cr substrates suggested that some regions of NiO remained present, which implies that complete removal of the NiO layer does not occur.

In contrast to NiO, the Cr_2O_3 portion of the oxide on the Ni–Cr substrates was largely unaffected by 20 min holding at the brazing temperature. Islands of Cr_2O_3 (Fig. 2) were observed on the substrate surface, and the extent of these increased with chromium content to the point where, on the 20% Cr substrate, a continuous Cr_2O_3 layer was produced.

In summary, these results indicate that holding at the brazing temperature results in the partial removal of NiO, whereas Cr_2O_3 remains stable.

3.1.3. Deoxidation mechanisms

Lugscheider *et al.* [8, 9] proposed two mechanisms for the decomposition of oxide layers on steels and nickel-based alloys during vacuum exposure, namely vaporization of the oxide and reduction by carbon originally present in the substrate. Consider first the NiO layer. The vapour pressure of NiO rises from 1.91×10^{-8} mbar at 1000 °C to 1.98×10^{-6} mbar at 1150 °C [10]. Thus whilst vaporization might significantly contribute to deoxidation at the higher temperatures, this process will be less important in the 1065 °C tests. Consider instead, reduction of the oxide layer by carbon originally present in solid solution in the substrate to produce metallic nickel and carbon monoxide. It is difficult to produce convincing experimental evidence for this process because the formation of carbon-containing phases can also be readily attributed to contaminant effects. Thus, to examine

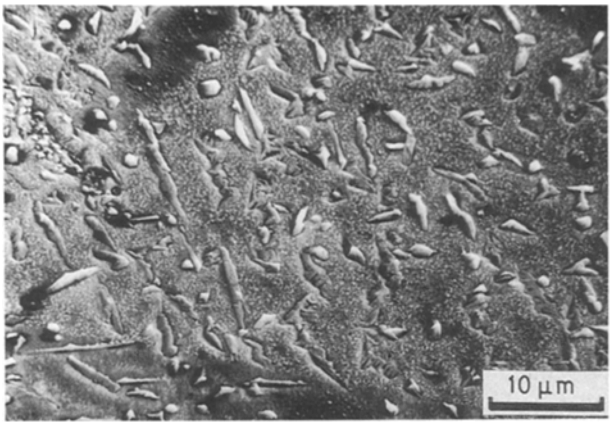

Figure 2 Oxide layer on Ni–10% Cr after heating to 1065 °C in a 7×10^{-5} mbar vacuum and holding for 20 min.

further this mechanism, consider instead the thermodynamics and kinetics of the process.

For the reaction

$$\mathrm{NiO} + \mathrm{C} = \mathrm{Ni} + \mathrm{CO} \qquad (1)$$

the equilibrium condition, assuming that the original oxide layer and the nickel formed from the reaction have unit activities, is given by

$$\Delta G^0 = -RT\ln\left(\frac{p_{\mathrm{CO}}}{a_{\mathrm{C}}}\right) \qquad (2)$$

for which ΔG^0 is the equilibrium Gibbs energy of reaction at the brazing temperature, T, R is the gas constant, p_{CO} the equilibrium partial pressure of carbon monoxide (in bar); and a_{C} the activity of carbon. Using the above equation and a carbon activity in the nickel substrate of 7×10^{-5} (based on the assumption that Raoult's law applies for a dilute solution of carbon in a nickel substrate), the maximum partial pressure of carbon monoxide that will allow the reaction to proceed (i.e. p_{CO}) is 598 mbar, at a temperature of 1000 °C. Because vacuums of 7×10^{-5} to 5×10^{-6} mbar were used experimentally, reduction of the oxide layer by carbon to form nickel and carbon monoxide is possible thermodynamically.

The kinetics of the reaction (which were not considered by Lugscheider *et al.* [8, 9]) are now examined. The following processes are capable of controlling the rate of reduction:

(a) development of a stagnant gaseous boundary layer (of carbon monoxide) in the furnace atmosphere above the sample;

(b) entrapment of carbon monoxide at the substrate metal–oxide interface;

(c) diffusion of carbon from the bulk substrate to the oxide surface.

Of these processes, adaption of the model for reaction control by the presence of gaseous boundary layers (developed by Graham and Davis [11] and based on data from Schwerdtfeger and Turkdogan [12]) for the oxidation of $\mathrm{Cr_2O_3}$ to gaseous $\mathrm{CrO_3}$ suggests that reduction will not be impeded by the production of a stagnant boundary layer, as might be expected for a pumped vacuum system.

Consider instead entrapment of the gaseous reaction products at the reaction site. At first sight, any reduction of the oxide taking place at the oxide–substrate metal interface would result in the formation of a carbon monoxide layer that might be trapped by the remaining oxide. However, because real oxide films contain pores and (in the case of vacuum-grown films) numerous cracks [13], this mechanism does not seem likely.

Lastly, it is necessary to consider whether the NiO reduction is controlled by carbon diffusion from the bulk substrate to the reaction layer. For a unit area of substrate oxide–metal interface, the total number of moles, n_{i}, of carbon that arrive at the metal–oxide interface in time t is given by

$$n_i = n_0 - n_{\mathrm{r}} \qquad (3)$$

i.e.

$$n_{\mathrm{i}} = c_0 x_{\mathrm{s}} - \int_0^{x_{\mathrm{s}}} c(x)\mathrm{d}x \qquad (4)$$

where n_0 is the number of moles of carbon originally present in the substrate, n_{r} the number of moles of carbon remaining in the substrate after time t, c_0 the initial carbon concentration in the substrate, x_{s} the thickness of the substrate, and $c(x)$ = concentration of carbon in the substrate as a function of distance x from the substrate metal–oxide interface at a constant time, t.

If carbon diffusion in the substrate is rate controlling (as is assumed here) then any carbon arriving at the substrate metal–oxide interface can be assumed to be immediately "removed" by reaction. If the thickness of the substrate is great enough so that the composition of the substrate at $x = x_{\mathrm{s}}$ (i.e. at the opposite face of the sample for a sample with a single oxidized surface) remains constant, then a simple decarburization model for a semi-infinite substrate [14] can be used in which

$$c(x) = c_0\,\mathrm{erf}\left(\frac{x}{2(Dt)^{1/2}}\right) \qquad (5)$$

where D is the carbon diffusivity in the substrate.

Assuming a hold time of 20 min and a diffusivity of $3.11 \times 10^{-11}\,\mathrm{m^2\,s^{-1}}$ (diffusivity of carbon in pure nickel at 1273 K [15]), it is found that, at a depth of 1 mm (i.e. the thickness of the substrate), the carbon concentration in the substrate is unchanged. Therefore, the use of this model is valid, because the substrate can be treated as semi-infinite. In order to integrate $c(x)$ (and then use it in Equation 4), a third order polynomial was fitted to Equation 5 between limits of $x = 0$ and $x = 1$ mm. By integrating this polynomial, it was found that, after 20 min at 1000 °C (with an original substrate carbon content of 7×10^{-3} at %), 2.3×10^{-3} mol carbon, n_{i}, diffuse from the bulk to each square metre of substrate metal–oxide interface. This can be compared with the number of moles of nickel oxide present, i.e. $8.9 \times 10^{-3}\,\mathrm{m^{-2}}$ of substrate surface (for a 100 nm thick oxide; based on interference colour observations [16] and studies of oxidation in vacuum brazing [17]). Because 1 mol carbon is required per 1 mol nickel oxide for the reduction reaction given in Equation 1, it is evident that sufficient carbon arrives at the substrate metal–oxide interface to deoxidize approximately one-quarter of the thickness of the oxide layer during the brazing. Hence, it would be expected that only partial deoxidation of NiO can occur during the brazing cycle and this correlates well with the experimental observations of the change in oxide thickness during vaccum exposure.

Turn now to the Cr_2O_3 formed on a Ni–20% Cr substrate. For the reaction

$$Cr_2O_3 + 3C = 2Cr + 3CO \tag{6}$$

it is possible to estimate the maximum partial pressure of carbon monoxide at which this reaction will occur (using the method employed for the reduction of NiO) as 6.89×10^{-5} mbar. Thus, reduction of Cr_2O_3 should also be possible thermodynamically. The failure to observe this process experimentally may be associated with the kinetic considerations described above for NiO, although more detailed characterization of the oxides present on the Ni–Cr substrates is required before the model developed for NiO can be applied.

In addition to reduction of the substrate Cr_2O_3, an alternative deoxidation mechanism proposed by Lugscheider *et al.* [8, 9] namely vaporization of the oxide layer in vacuum, needs to be considered. There is a lack of systematic vapour pressure data for Cr_2O_3. However, the study of Lugscheider *et al.* suggests that significant vaporization of bulk Cr_2O_3 first occurs at temperatures of between 950 and 1000 °C under a 10^{-5} mbar vacuum. In contrast, in the present investigation, the Cr_2O_3 layer remained present during holding at temperatures of up to 1150 °C in a vacuum of 5×10^{-6} mbar. This could be due to continual reoxidation of the surface.

In summary, both NiO and Cr_2O_3 form during heating to the brazing temperature, although the NiO partially decomposes during subsequent holding at the brazing temperature. This decomposition of the NiO is consistent with deoxidation by carbon originating from the substrate and so the rate of deoxidation will be controlled by the rate of carbon diffusion in the substrate. Because decomposition of the NiO occurs only after holding at temperature, it will be of importance only in the later stages of the filler spreading process (see Section 3.4).

3.2. Oxide reduction by filler constituents

In contrast to the general deoxidation processes described above, consider now localized reduction of the oxide in contact with and around a filler droplet. Both boron and silicon present in the filler are capable thermodynamically of reducing NiO and Cr_2O_3 by the following reactions (if it is assumed that the products of the reaction have unit activity, and boron and silicon obey Raoult's law when in solution in nickel)

$$NiO + \tfrac{2}{3}B = Ni + \tfrac{1}{3}B_2O_3$$

$$\Delta G_{1373\,K} = -171\ \mathrm{kJ\,mol^{-1}} \tag{7}$$

$$Cr_2O_3 + 2B = 2Cr + B_2O_3$$

$$\Delta G_{1373\,K} = -106\ \mathrm{kJ\,mol^{-1}} \tag{8}$$

$$NiO + \tfrac{1}{2}Si = Ni + \tfrac{1}{2}SiO_2$$

$$\Delta G_{1373\,K} = -198\ \mathrm{kJ\,mol^{-1}} \tag{9}$$

$$Cr_2O_3 + \tfrac{3}{2}Si = 2Cr + \tfrac{3}{2}SiO_2$$

$$\Delta G_{1373\,K} = -187\ \mathrm{kJ\,mol^{-1}} \tag{10}$$

Experimentally, however, it was found that reduction of the substrate oxide layer was achieved only by boron and reduction by silicon did not take place. Depth profiling using LAMMS revealed that the region of reduced oxide was enriched in boron and deficient in silicon when compared to the main sample. In addition, using XRD, the boron oxide phases B_2O_3 and B_6O were detected. However, the B_2O_3 could be identified only in furnace-cooled specimens, presumably because this phase is normally vitreous (i.e. has a non-crystalline structure) [18, 19] and hence would not be detected by XRD in fast-cooled samples. The occurrence of the boron-rich B_6O suboxide might be attributed to a large excess of boron compared to oxygen due to the relatively small amount of residual oxide.

In order to understand the reasons for reduction by boron rather than silicon, consider first thermodynamic factors. The assumptions regarding activities made at the start of this section may not apply in practice. For example, B_2O_3 is mutually soluble with the oxide layers on nickel-based alloys [20], and hence the activity of B_2O_3 may differ substantially from unity and the reactions in Equations 7 and 8 would become more favourable. However, any changes in activities of NiO and Cr_2O_3 would also need to be considered.

Turn instead to kinetic factors. It was observed experimentally that the process of spreading of Ni–Si–B filler droplets occurred in two distinct stages, namely an initial rapid stage and a slower subsequent stage. The nature of reduction of the substrate oxide during these two stages is now considered.

During the initial rapid spreading stage, reduction of part of the substrate oxide layer by boron takes place at the spreading front, whilst any remaining unreduced oxide is carried on to the surface of the liquid droplet and then reduced (Fig. 3a). Long-range solid-stage diffusion is not required and so a kinetic explanation to account for the observed reduction by boron rather than silicon is not probable.

During the second slower spreading stage, reduction of the substrate oxide by boron occurs ahead of the substrate–filler interface (Fig. 3b). In this case, long-range diffusion of the reactants from the filler droplet to the reaction site is required and kinetic factors could be of importance. Assuming diffusion control of the reaction, the rate of increase in radius of the reaction zone can be determined using the approximation

$$x \approx (Dt)^{1/2} \tag{11}$$

where x is the width of the reaction layer, D is the diffusivity of the reactant and t is holding time. Using data from Fig. 4 (in which regions are observable where the width of the reaction layer around the braze droplet apparently decreases; these regions are in fact

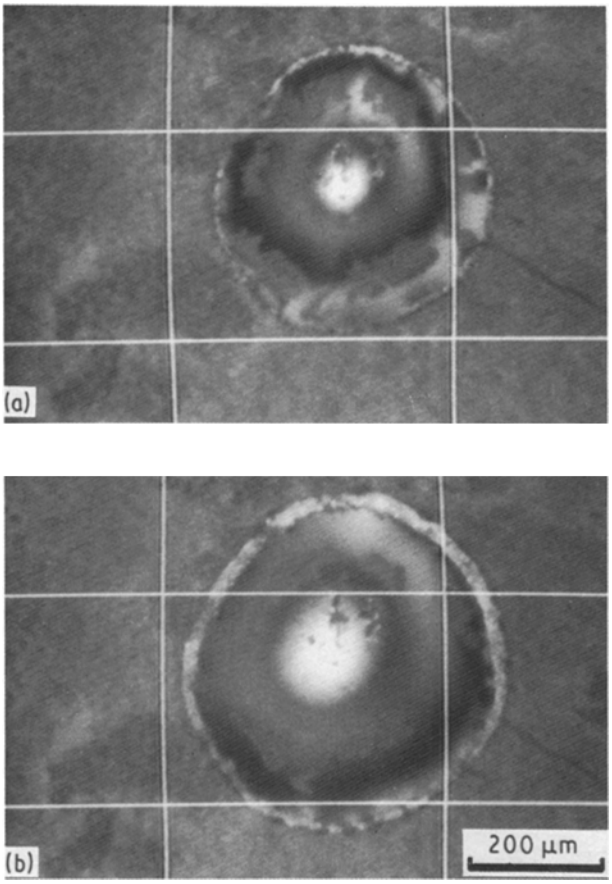

Figure 3 Location of substrate oxide reduction front (preoxidized substrate, tested at 1150 °C, 10^{-5} mbar). (a) Initial stage (5 s after melting) oxide reduction front at filler–substrate interface); (b) later stage (10 s after melting) oxide reduction front in the substrate ahead of filler–substrate interface.

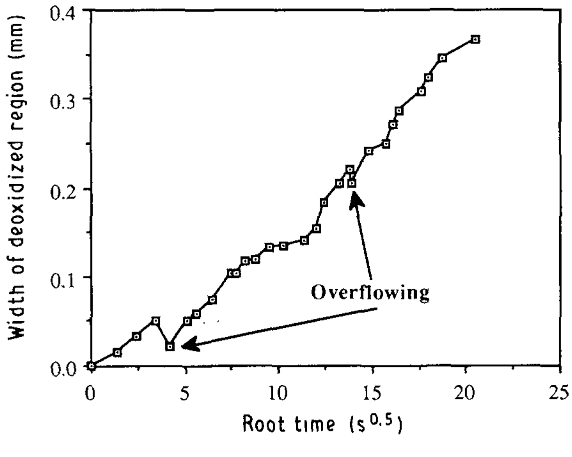

Figure 4 Development of a deoxidized region around a filler droplet on a Ni–10% Cr substrate (tested at 1150 °C in a 10^{-5} mbar vacuum).

due to overflowing of the filler, i.e. spreading into the reaction layer, which effectively reduces its width), a value for D of $3.5 \times 10^{-10}\,m^2\,s^{-1}$ was obtained. This value might reasonably be associated with diffusion in the solid state because it is lower than would be expected for diffusion through a liquid (in this case, the layer of liquid B_2O_3 on the substrate surface ahead of the filler droplet) for which diffusivity values of around $10^{-8}\,m^2\,s^{-1}$ would be expected. However, it is not possible to determine the extent to which this observation indicates that the reduction reaction by boron takes place under boron diffusion control (note that the bulk diffusivity of boron in nickel is $6.22 \times 10^{-11}\,m^2\,s^{-1}$ [21]).

In summary, evidence has been presented that two reaction regimes occur. Firstly, whilst the filler is spreading rapidly, reduction of the substrate oxide takes place in contact with the surface of the filler droplet. Secondly, once rapid spreading has ceased, reaction takes place ahead of the main filler droplet. In both cases, the reduction reaction is dominated by boron (only oxides of boron were observed experimentally). In the next two sections, the role of these reduction reactions in the overall spreading of the filler will be considered.

3.3. Oxide reduction and the onset of isothermal solidification

In earlier work [5], it was proposed that the onset of isothermal solidification controls the final extent of spreading and that isothermal solidification is hastened by boron removal from the filler metal during reduction of the substrate oxide layer. The role of the isothermal solidification process is clearly evident in Figs 5a and 6 (which is an extreme example using a preoxidized substrate); the point at which rapid spreading ceases (point A in the figures) corresponds to the onset of isothermal solidification at the edge of the filler droplet. However, in order to examine the onset of isothermal solidification, consideration of the role of oxide reduction in the isothermal solidification process is necessary. Note that, during this early stage of the spreading process, the generalized deoxidation mechanisms described in Section 3.1 do not have a significant effect.

In Section 3.2, evidence has been presented to show that boron emanating from the filler can reduce the substrate oxide and that the silicon in the filler metal plays no apparent part in the oxide reduction process. Thus, when considering the possible effects of substrate oxide reduction on isothermal solidification in this paper, only boron is considered. Suppose that oxide reduction can be described by Equation 7. In this case, for every mole of nickel oxide reduced, 2/3 mol boron are consumed. Thus the number of moles of boron, Δn_B, depleted from the filler during reduction is given by

$$\Delta n_B = \frac{2}{3} n_{OX} = \frac{2}{3} \frac{\rho V}{M} \qquad (12)$$

where n_{OX} is the number of moles of substrate oxide [NiO] reduced by the filler during spreading, ρ the density of the oxide, V the volume of oxide reduced by the filler, and M the molar mass of the oxide. If reduction takes place at the filler–substrate oxide interface, the filler makes contact with a unit area of oxide for each unit area of substrate spread over. The volume of oxide reduced by the filler in a given time Δt can be obtained from

$$V = \pi R_F^2 l = \pi (R_0 + \Delta R)^2 l \qquad (13)$$

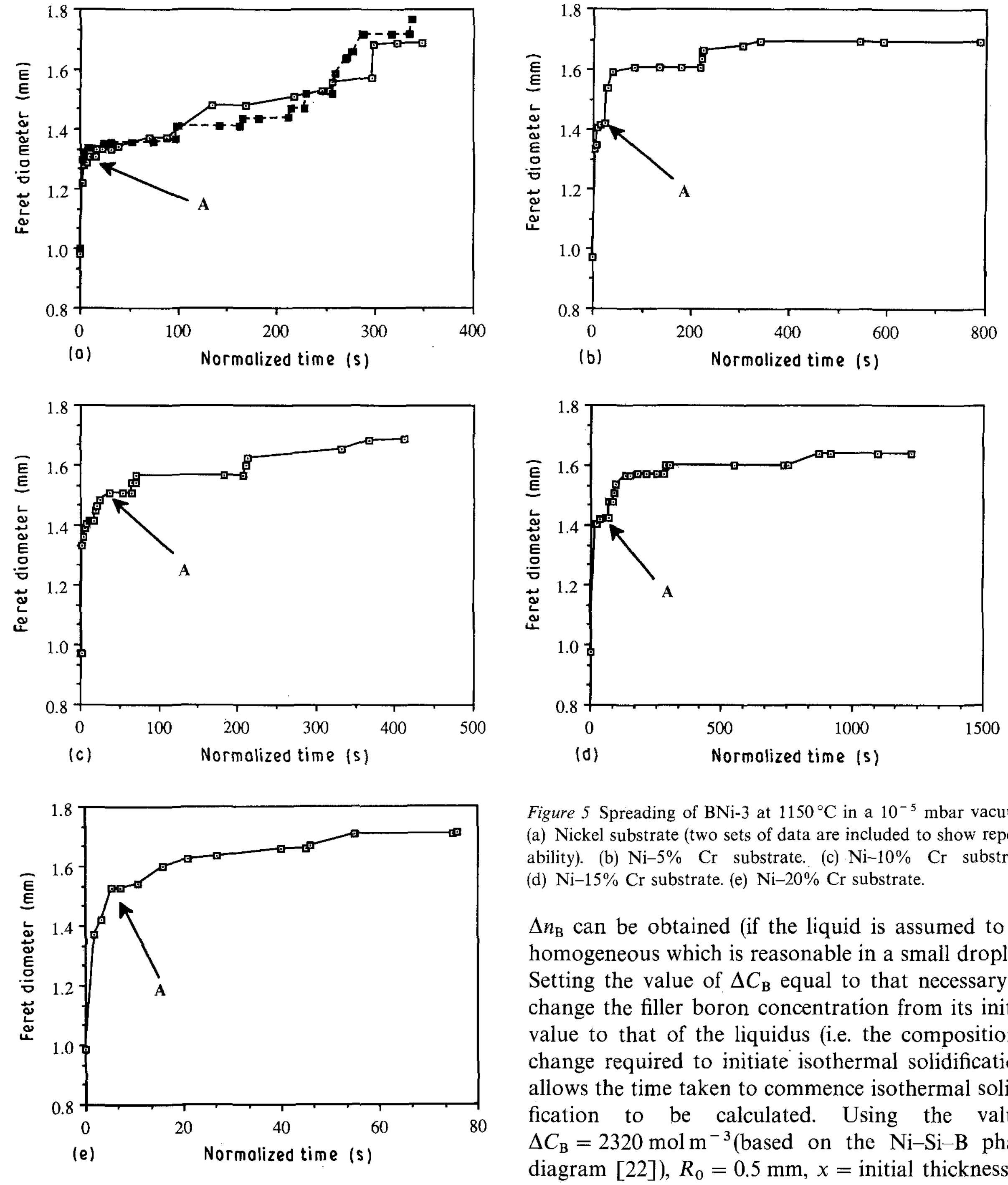

Figure 5 Spreading of BNi-3 at 1150 °C in a 10^{-5} mbar vacuum. (a) Nickel substrate (two sets of data are included to show repeatability). (b) Ni–5% Cr substrate. (c) Ni–10% Cr substrate. (d) Ni–15% Cr substrate. (e) Ni–20% Cr substrate.

where R_F is the final radius of the droplet, l the thickness of the oxide layer on the substrate, R_0 the initial radius of the droplet, and ΔR the increase in radius of the droplet during spreading.

Experimentally it was found that, before the onset of isothermal solidification, the rate at which the radius of the droplet increased, ν, was approximately constant so that

$$\Delta R = \nu \Delta t \qquad (14)$$

where Δt is the time elapsed since the commencement of spreading. By substituting for ΔR in Equation 13 and inserting the resulting value for V into Equation 12, it is possible to obtain the amount of boron depletion, Δn_B, as a function of time. Assuming that before the onset of isothermal solidification, the volume of liquid remains constant, the change in the concentration of boron in the liquid ΔC_B, induced by Δn_B can be obtained (if the liquid is assumed to be homogeneous which is reasonable in a small droplet). Setting the value of ΔC_B equal to that necessary to change the filler boron concentration from its initial value to that of the liquidus (i.e. the compositional change required to initiate isothermal solidification) allows the time taken to commence isothermal solidification to be calculated. Using the values $\Delta C_B = 2320\ \text{mol m}^{-3}$(based on the Ni–Si–B phase diagram [22]), $R_0 = 0.5$ mm, x = initial thickness of the braze disc = 51 μm, l = 100 nm (see Section 3.1), $\nu \approx 5 \times 10^{-4}\ \text{m s}^{-1}$ (determined experimentally using hot-stage light microscopy for BNi-3 on a nickel substrate), $\rho = 6670\ \text{kg m}^{-3}$, and $M = 74.71$ g, it is found that the filler should attain the liquidus composition and begin to solidify after 3.5 s. Note that it has been assumed in this calculation that boron removal from the filler is dominated during the initial rapid stage of spreading by oxide reduction and that interdiffusion has been neglected.

In order to compare the above prediction with experiment, consider Fig. 5a which shows plots of the average diameters of BNi-3 droplets on nickel substrates as a function of holding time. It can be seen that there are two spreading regimes. The first of these regimes involves a brief rapid spreading stage (0–A on Fig. 5a) during which spreading is almost linear with respect to time. This rapid stage is followed by a protracted stage involving much slower spreading in

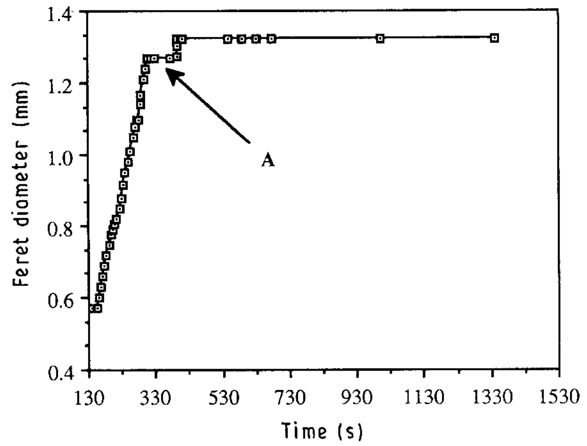

Figure 6 Spreading of BNi-3 on a preoxidized Ni–5% Cr substrate (tested at 1150 °C in a 10^{-5} mbar vacuum).

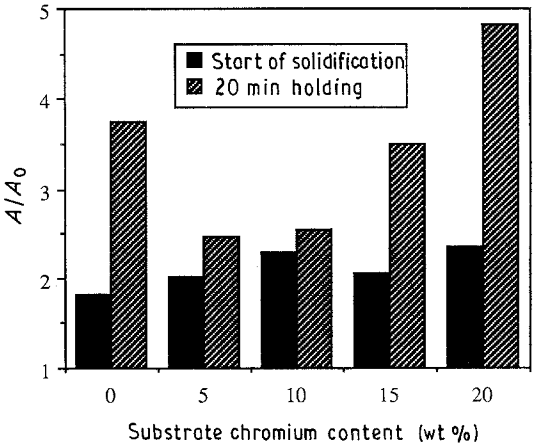

Figure 7 Comparison of extent of spreading at the onset of isothermal solidification (hot stage) and after 20 min at 1150 °C (sessile drop) in a 10^{-5} mbar vacuum (A = area of the spread droplet, A_0 = area of initial punched out disc of filler).

a stepwise fashion. The transition between the two regimes (point A) was observed to correspond with the onset of isothermal solidification and this occurred after 1.25–2.5 s. This range is similar to the theoretical prediction above. However, further corroboration is obviously desirable and so the spreading of BNi-3 on a preoxidized substrate was also examined (Fig. 6). For the preoxidized substrate, two factors change. Firstly, the amount of oxide that has to be reduced per unit area spread over by the filler is increased (due to the increase in oxide thickness from around 100 nm to around 700 nm) and, secondly, the spreading rate is decreased (from 5.0×10^{-4} to 2.3×10^{-6} m s^{-1}). Of these two factors, the former should hasten and the latter delay the onset of isothermal solidification. When a predicted Δt value is calculated, it is found that the effect of the reduced spreading velocity predominates and a Δt value of 148 s is obtained. This value is in good agreement with that of around 150 s obtained experimentally.

In summary, a simple model has been presented that successfully predicts the time required before the onset of isothermal solidification. The model is based solely on the removal of boron from the filler during oxide reduction. The success of the model suggests that in the case of spreading droplets it is the reduction process, rather than diffusion into the substrate, that leads to the onset of isothermal solidification. Note, however, that this will not be the case for the completion of isothermal solidification which is an important factor in TLP bonding.

3.4. Anomalous spreading behaviour at high temperatures

In the previous section, the role of oxide reduction in the initial rapid spreading stage was considered. During this stage, spreading is dependent upon oxide reduction arising from direct contact with the filler metal. However, if the second slower spreading stage (that follows the onset of isothermal solidification) produces a significant extent of spreading, both oxide reduction ahead of the filler droplet and generalized deoxidation will also need to be considered.

In spreading tests conducted at 1065 and 1110 °C, the onset of isothermal solidificaton was found effectively to terminate spreading. However, in tests conducted at 1150 °C (Fig. 5a–e), the remaining liquid is relatively fluid and spreading can continue after the onset of isothermal solidification (points A on the figures). This spreading involves liquid filler flowing over the resolidified edge of the filler droplet and this occurs in a stepwise manner. Each step corresponds to overflowing of the solid edge of the droplet followed by solidification of the flowing liquid.

Overflowing generally takes place into the reaction zone around the liquid droplet where the substrate oxide has already been reduced. Thus, depletion of boron due to oxide reduction will not occur and so cannot contribute to the onset of isothermal solidification of the overflowing liquid. Furthermore, even when the overflowing liquid spreads beyond the reaction zone into the oxidized portion of the substrate, the vacuum deoxidation that occurs during holding at temperature (see Section 3.1) should reduce (or modify) the influence of the substrate oxide on the spreading of the filler. Thus the spreading arising from overflowing is expected to be different from that described earlier.

Experimentally, it was found that overflowing modifies the trend in spreading with substrate chromium content. At the end of the initial spreading stage, the trend in the extent of spreading at the onset of isothermal solidification with substrate chromium content (Fig. 7) is similar to that of the final extent of spreading at lower temperatures (as discussed previously [5]). This trend can be attributed to changes in the nature of the substrate oxide with the addition of chromium to the substrate [5]. However, the trend in spreading with substrate chromium content becomes different in the overflowing stage (Fig. 7). Thus, while the model for the termination of the initial spreading stage described in Section 3.3 is still valid at 1150 °C, the final extent of spreading is markedly influenced by the second spreading stage.

4. Conclusions

An investigation has been made of the interaction between substrate oxide reduction, isothermal solidification and the spreading of Ni–Si–B fillers. As a result of this study, a number of conclusions can be drawn.

1. Decomposition of the substrate oxide layers as a result of high-temperature vacuum exposure occurs only to a limited extent during the complete brazing cycle. An analysis of the kinetics of the decomposition process is consistent with reduction by carbon emanating from the substrate.
2. Localized reduction of the substrate oxide in the vicinity of the filler droplet is produced by boron originally present in the braze metal.
3. A model for the control of spreading by the onset of isothermal solidification as a consequence of boron removal from the filler during substrate oxide reduction is in agreement with experimental results.
4. At higher brazing temperatures (1150 °C), significant spreading occurs after the onset of isothermal solidification; however, the model for the onset of isothermal solidification remains valid.

Acknowledgements

The authors thank Mrs J. C. Ambrose and Dr M. G. Nicholas, A.E.A. Technology (Harwell), for their cooperation. A number of useful discussions with Professor H. Nakae, Wasseda University, Japan and Dr S. Kuroda, National Research Institute for Metals, Japan, are gratefully acknowledged. Rapidly solidified brazing alloys were kindly provided by Neomet Ltd, Stockport. The project was financially supported by A.E.A. Technology and the Science and Engineering Research Council.

References

1. D. S. DUVALL, W. A. OWCZARSKI and D. F. PAULONIS, *Weld. J.* **53** (1974) 203.
2. I. TUAH-POKU, M. DOLLAR and T. B. MASSALSKI, *Metall. Trans.* **19A** (1988) 575.
3. Y. NAKAO, K. K. NISHIMOTO, K. SHINOZAKI and C. KANG, "Transient Insert Metal Diffusion Bonding of Ni-Base Cast Superalloy MM007" (International Institute of Welding, London, UK, 1986).
4. Y. NAKAO, K. K. NISHIMOTO, K. SHINOZAKI and C. KANG, in "Superalloys 1988" (Metallurgical Society of AIME, PA, 1989).
5. W. F. GALE and E. R. WALLACH, *Weld. J.* (*Res. Suppl.*) **70** (1991) 76s.
6. L. L. SHREIR, "Corrosion", Vol. 1 (Newnes-Butterworths, London, 1976) p. 7.82.
7. W. Z. FRIEND, "Corrosion of Nickel and Nickel-Base Alloys" (Wiley Interscience, New York, 1980) p. 163.
8. E. LUGSCHEIDER and H. ZHUANG, *Schweissen Schneiden* **34** (1982) 490.
9. E. LUGSCHEIDER, H. ZHUANG and M. MAIER, *Weld. J.* (*Res. Suppl.*) **62** (1983) 295s.
10. F. D. ROSSINI, D. D. WAGMAN, W. H. EVANS, S. LEVINE and I. JAFFE, "Selected Values of Chemical Thermodynamic Properties" (US Government Printing Office, Washington DC, 1952) p. 690.
11. H. C. GRAHAM and H. H. DAVIS, *J. Amer. Ceram. Soc.* **54** (1971), 89.
12. K. SCHWERDTFEGER and E. T. TURKDOGAN, in "Physiochemical Measurements in Metals Research" Vol. 4, edited by R. A. Rapp (Wiley Interscience, New York, 1970) p. 322.
13. W. F. GALE and E. R. WALLACH, International University Seminar on Brazing, Aachen, FRG, September 1990, *Schweißen Schneiden* **43** (1991) 386 (E. 143).
14. J. CRANK, "The Mathematics of Diffusion", 2nd Edn (Oxford University Press, Oxford, 1975).
15. E. A. BRANDES (Ed.), "Smithells Metals Reference Book", 6th Edn (Butterworths, London, 1983) p. 8.21.
16. F. HURN-CONSTABLE, *Proc. R. Soc.* **117** (1928) 376.
17. J. M. COHEN, J. E. CASTLE and M. B. WALDRON, *Metal. Sci.* **15** (1981) 455.
18. N. P. NIES and G. W. CAMPBELL, in "Boron, Metallo-Boron Compounds and Boranes", edited by R. M. Adams (Wiley Interscience, New York, 1964) p. 53.
19. N. N. GREENWOOD, "The Chemistry of Boron" (Pergamon Press, Oxford, 1973) p. 880.
20. D. ROLLER and C. R. ANDREWS, *Corrosion NACE* **15** (1959) 49.
21. J. KUCERA, A. BUCHAL, A. REK and K. STRANSKY, *Kovove Mater.* **22** (1984) 250.
22. S. ÔMORI, Y. HASHIMOTO, K. SHÔJI, K. HADAKA and Y. KOHIRA, *J. Jpn Soc. Powder Metall.* **18** (1972) 316.

Received 23 July
and accepted 30 July 1991